THE JOURNAL OF BIOLOGICAL CHEMISTRY
Vol. 270, No. 50, Issue of December 15, pp. 30194–30198, 1995
Printed in U.S.A.

Structure-specific Nuclease Activity in Yeast Nucleotide Excision Repair Protein Rad2*

(Received for publication, August 3, 1995, and in revised form, October 11, 1995)

Yvette Habraken, Patrick Sung, Louise Prakash, and Satya Prakash‡

From the Sealy Center for Molecular Science, University of Texas Medical Branch, Galveston, Texas 77555-1061

***Saccharomyces cerevisiae* Rad2 protein functions in the incision step of the nucleotide excision repair of DNA damaged by ultraviolet light. Rad2 was previously shown to act endonucleolytically on circular single-stranded M13 DNA and also to have a 5′ → 3′ exonuclease activity (Habraken, Y., Sung, P., Prakash, L., and Prakash, S. (1993) *Nature* 366, 365–368; Habraken, Y., Sung, P., Prakash, L., and Prakash, S. (1994) *J. Biol. Chem.* 269, 31342–31345). Using two different branched DNA structures, pseudo Y and flap, we have determined that Rad2 specifically cleaves the 5′-overhanging single strand in these DNAs. Rad2 nuclease is more active on the flap structure than on the pseudo Y structure. Rad2 also acts on a bubble structure that contains an unpaired region of 14 nucleotides, but with a lower efficiency than on the pseudo Y or flap structure. The incision points occur at and around the single strand-duplex junction in the three classes of DNA structures.**

Nucleotide excision repair (NER)[1] of UV-damaged DNA in eukaryotes occurs by dual incision of the damaged DNA strand (1). Genetic and biochemical studies in the yeast *Saccharomyces cerevisiae* have indicated the requirement for a large number of protein factors in NER (2, 3). Reconstitution of the incision step of NER requires the DNA damage binding protein Rad14, the Rad4-Rad23 complex, the Rad1-Rad10 nuclease, the Rad2 nuclease, the three-subunit replication protein A, and the six-subunit pol II transcription factor TFIIH (3). The Rad1-Rad10 and Rad2 nucleases mediate dual incision of the damaged DNA strand, releasing excision DNA fragments of 24–27 nucleotides in length (3).

The Rad2 nuclease is related to the *Escherichia coli* pol I 5′ → 3′ exonuclease in that these enzymes share homology in domains conserved in pol I and related microbial nucleases. The *E. coli* 5′ → 3′ nuclease functions in the removal of RNA primers from the newly synthesized DNA strand. The temperature-sensitive *polA ex1* mutant of *E. coli* is defective in the 5′ → 3′ nuclease activity, and joining of Okazaki fragments is retarded in this mutant (4). In addition to containing a 5′ → 3′ exonuclease activity, the pol I nuclease exhibits a structure-specific activity that cleaves the 5′-end single-stranded DNA or RNA at its junction with the duplex DNA (5).

A mammalian 45-kDa 5′ → 3′ exonuclease that is related to *E. coli* pol I 5′ → 3′ nuclease and that shares homology with yeast Rad2 is required for lagging strand DNA synthesis in reconstituted DNA replication systems (6–10). Following the RNase H1-catalyzed cleavage of primer RNA one nucleotide 5′ of the RNA-DNA junction, the 5′ → 3′ exonuclease removes the remaining monoribonucleotide of the RNA primer (9). Like the pol I nuclease, the mammalian enzyme also has a similar structure-specific activity (11). The *RTH1* gene encodes the *S. cerevisiae* counterpart of this mammalian 45-kDa exonuclease (12). Genetic studies with the *rth1*Δ mutant strain have indicated a role of RTH1 in DNA replication as well as in DNA mismatch repair (12, 13).

The protein encoded by *RTH1* and its mammalian counterpart contains ~380 amino acids. Rad2, by contrast, is a much larger protein, containing 1031 residues. The homology between yeast Rad2, RTH1, and their mammalian counterparts is restricted to three regions (for references, see Ref. 12). Moreover, whereas RTH1 and its mammalian counterparts have a role in DNA replication and in mismatch repair, Rad2 is required for NER, but has no apparent involvement in DNA replication and mismatch repair (2, 3, 12).[2] Thus, Rad2 and RTH1 proteins have diverged functionally. Here, we examine the action of Rad2 nuclease on various DNA structures.

MATERIALS AND METHODS

Purification of Rad2 Protein—Rad2 protein was purified from the protease-deficient yeast strain LY2 (*MATα*, *gal1*, *reg1-501*, *leu2-3*, *leu2-114*, *ura3-52*, *trp1*Δ, *pep4-3*, *prb1-112*) harboring the Rad2-overproducing plasmid pR2.26. In pR2.26, the *RAD2* gene is under the control of the synthetic hybrid *GAL-PGK* promoter inducible by galactose (14). Starting from crude lysate prepared from 200 g of LY2(pR2.26), we used a combination of ammonium sulfate precipitation and chromatographic fractionation on columns of Q-Sepharose, S-Sepharose, Sephacryl S-300, and Mono S to obtain ≈100 μg of nearly homogeneous Rad2 protein (14). Purified Rad2 protein was concentrated to 400 μg/ml using a Centricon-30 microconcentrator (Amicon, Inc.) and stored in small portions at −70 °C. Once thawed, the Rad2 protein solution was kept on ice, where it remains enzymatically active for at least 1 week.

Polyclonal Antibodies Specific for Rad2—A β-galactosidase-Rad2 fusion protein was expressed in *E. coli* carrying the plasmid pKM8 (14). The insoluble hybrid polypeptide was purified from inclusion bodies by preparative SDS-polyacrylamide gel electrophoresis and used as antigen for polyclonal antibody production in rabbits. Antibodies were affinity-purified from the rabbit sera by passage through a Sepharose column containing the covalently linked antigen. After dialysis against phosphate-buffered saline (10 mM NaH_2PO_4, pH 7.2, 150 mM NaCl), the antibody solution was concentrated to 2 mg/ml and stored in small portions at −70 °C. Affinity-purified polyclonal antibodies specific for Rad1 and Rad10 proteins were obtained as described previously (15).

Oligonucleotides Used—The following oligonucleotides were used to construct various DNA substrates. Oligonucleotide A, which contains 50 bases, has the sequence 5′-GGGACTGGACTTGCCGACTTTGACTTGACTGGCTGTGGACTTTTTGGGGG-3′. Oligonucleotide B, a 20-mer, has the sequence 5′-CCCCCAAAAAGTCCACAGCC-3′. Oligonucleotide C, a 50-mer, has the sequence 5′-ATGGTGTATAGCAATGT-

* This work was supported by Grant CA35035 from the National Cancer Institute and Grant DE-FGO3-93ER61706 from the Department of Energy. The costs of publication of this article were defrayed in part by the payment of page charges. This article must therefore be hereby marked "*advertisement*" in accordance with 18 U.S.C. Section 1734 solely to indicate this fact.

‡ To whom correspondence should be addressed: Sealy Center for Molecular Science, University of Texas Medical Branch, 6.104 Medical Research Bldg., 11th & Mechanic St., Galveston, TX 77555-1061. Tel.: 409-747-8602; Fax: 409-747-8608.

[1] The abbreviations used are: NER, nucleotide excision repair; pol, polymerase.

[2] R. E. Johnson, L. Prakash, and S. Prakash, unpublished results.

TCTAGTCAAGTCAAAGTCGGCAAGTCCAGTCCC-3′. Oligonucleotide D, a 20-mer, has the sequence 5′-AAGTCGGCAAGTCCAGTCCC-3′. Oligonucleotide E, a 50-mer, has the sequence 5′-CCCCCAAAAAGTC-CACAGCCAGTCAAGTCACCTTCTTGTCGTTCACCCTT-3′. Oligonucleotide F, a 62-mer, has the sequence 5′-GGGTCAACGTGGGCAAA-GACCTCGTTTTTTTTTTTTTTGTGCAAGCCAGAATTGGGCAGG-TC-3′. Oligonucleotide G, a 62-mer, has the sequence 5′-GACCTGCCC-AATTCTGGCTTGCACTGTGTGTGTGTGTGCGAGGTCTTTGCCCA-CGTTGACCC-3′.

DNA Substrates—Oligonucleotides A, C, E, and G were radiolabeled at their 5′-terminus with the bacteriophage T4 polynucleotide kinase and [γ-^{32}P]ATP (Amersham Corp.; 6000 Ci/mmol). DNA substrates were obtained by annealing one of the radiolabeled oligonucleotides to nonlabeled oligonucleotides. Radiolabeled oligonucleotide C was hybridized to oligonucleotide A to generate the pseudo Y-1 substrate shown in Fig. 1, and radiolabeled oligonucleotide C was hybridized to oligonucleotides A and B to generate Flap-1, which contains a 5′-overhanging single strand (see Fig. 1). Radiolabeled oligonucleotide E was hybridized to oligonucleotide A and radiolabeled oligonucleotide E was hybridized to oligonucleotides A and D to generate the pseudo Y-2 and 3′-overhanging Flap-2 DNA substrates, respectively (see Fig. 1). To obtain the bubble DNA substrate (see Fig. 1), radiolabeled oligonucleotide G and oligonucleotide F were hybridized to each other. Annealing reactions were carried out by mixing 180 pmol of radiolabeled oligonucleotides with 200 pmol of nonradiolabeled oligonucleotides in 50 μl of buffer (50 mM Tris-HCl, pH 8.2, 10 mM $MgCl_2$, 0.2 mM EDTA, 5 mM dithiothreitol, and 0.1 mM spermidine) and incubating at 92 °C for 2 min, at 65 °C for 10 min, at 37 °C for 20 min, and finally at 25 °C for 20 min. Annealing mixtures were run at 4 °C on 8% polyacrylamide gels in TBE buffer (90 mM Tris borate, pH 8.5, 2 mM EDTA); the region of the gel containing the radiolabeled DNA substrate was excised; and the DNA was eluted by diffusion from the crushed gel slice at 4 °C overnight into TE buffer (10 mM Tris-HCl, pH 7.5, 1 mM EDTA, and 50 mM KCl). The purified DNA substrates were stored at 4 °C.

Nuclease Assay—Rad2 protein (2–40 ng or 17–340 fmol) was incubated with 75 fmol of 5′-^{32}P-labeled DNA (7,000–20,000 cpm) in reaction buffer (50 mM Tris-HCl, pH 8.0, 5 mM $MgCl_2$, 1 mM dithiothreitol, and 100 μg/ml bovine serum albumin) for 10 min at 30 °C in a final volume of 11 μl. The reaction was terminated by adding 11 μl of gel loading buffer (90% deionized formamide in TBE buffer); the mixture was heated for 2 min at 92 °C, and a fraction of it (2,500 cpm) was loaded on an 11% polyacrylamide gel containing 7 M urea and 16% formamide in TBE buffer. Electrophoresis was carried out for 2 h at 30 V/cm on 0.5-mm-thick polyacrylamide gels that had been prerun at the same constant voltage for 30 min. Gels were soaked in a mixture of 20% methanol and 5% acetic acid for 15 min before being dried. The gel was either subjected to autoradiography to visualize the radiolabeled substrates and products or analyzed in the PhosphorImager 425 (Molecular Dynamics, Inc.) to quantify the various radiolabeled DNA species. The size markers used were purchased from Pharmacia Biotech Inc. and were 5′-end-labeled with [γ-^{32}P]ATP and T4 polynucleotide kinase.

RESULTS

Specific Cleavage of Pseudo Y DNA Structure by Rad2 Protein—To determine whether the Rad2 nuclease activity would mediate the cleavage of a DNA structure that contains single-stranded tails adjacent to a duplex region, we hybridized ^{32}P-labeled oligonucleotide C to partially homologous and nonradiolabeled oligonucleotide A (see "Materials and Methods") to give the pseudo Y-1 substrate shown in Fig. 1. Reaction mixtures that contained Rad2 protein and pseudo Y-1 were incubated at 30 °C and then heated for 2 min at 95 °C in the presence of formamide to inactivate Rad2 protein and to separate the hybridized DNA strands. The mixture was then run, along with radiolabeled DNA size markers, on an 11% polyacrylamide gel containing 7 M urea and 16% formamide to prevent rehybridization of the DNA strands during electrophoresis. The gel was subjected to autoradiography to reveal the radiolabeled DNA species and was also analyzed in the PhosphorImager to quantify these species. The presence of DNA denaturants in the polyacrylamide gel enabled us to determine precisely the size of the cleavage products. As shown in Fig. 2 (*lanes 5–8*), Rad2 protein cleaved the ^{32}P-labeled 5′-overhanging single strand in pseudo Y-1 to yield two major

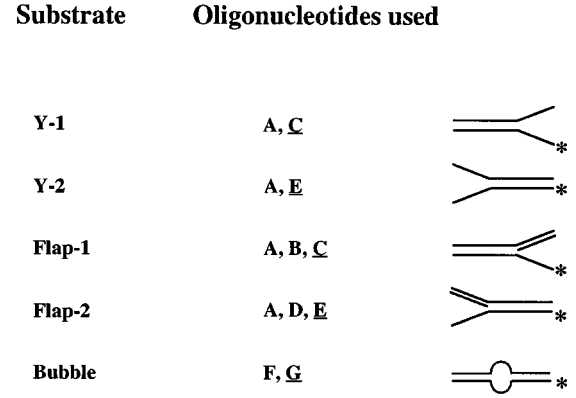

FIG. 1. **DNA substrates used.** *Asterisks* indicate the position of the 5′-^{32}P label, and the oligonucleotides that carry the label are *underlined*. The conditions used for annealing the oligonucleotides and other experimental details that pertain to the construction of the substrates are described under "Materials and Methods."

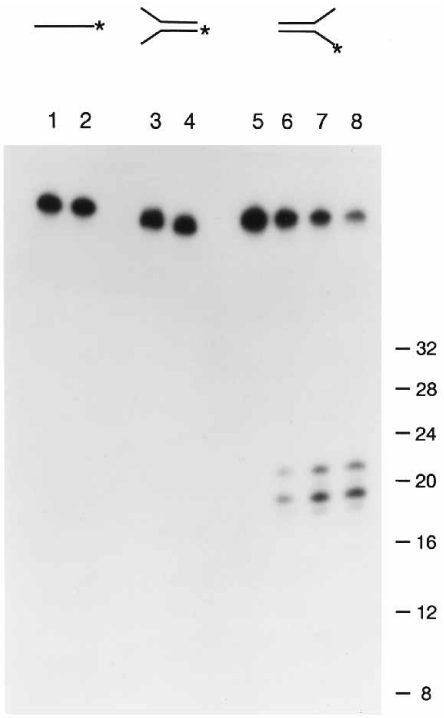

FIG. 2. **Rad2 nuclease specifically cleaves 5′-overhanging single-stranded tail in pseudo Y structure.** Radiolabeled oligonucleotide A (*lanes 1* and *2*), pseudo Y-2 (*lanes 3* and *4*), and pseudo Y-1 (*lanes 5–8*) (75 fmol each) were incubated without (*lanes 1*, *3*, and *5*) or with Rad2 protein (10 ng in *lane 6*, 15 ng in *lane 7*, and 20 ng in *lanes 2*, *4*, and *8*) for 10 min at 30 °C. The reaction mixtures were run on a 11% polyacrylamide gel followed by autoradiography to reveal the radiolabeled DNA species. The numbers to the right of the autoradiogram mark the positions in nucleotides of the mixture of size standards used.

products of 19 nucleotides (≈43% of total) and 21 nucleotides (≈32% of total) and two minor products of 18 nucleotides (12% of total) and 20 nucleotides (≈13% of total), as determined by PhosphorImager analysis of products in *lane 8*. The amount of these nucleolytic cleavage products was proportional to the quantity of Rad2 added to the reaction mixture (Fig. 2, *lanes 6–8*). Based on the sizes of these nucleolytic products, it can be deduced that the sites of cleavage in the radiolabeled strand in pseudo Y-1 by Rad2 protein range from 1 base into the duplex region to 2 bases away from the duplex region (see Fig. 6).

The cleavage reaction mediated by Rad2 protein is specific for the 5′-overhanging single-stranded tail in the pseudo Y

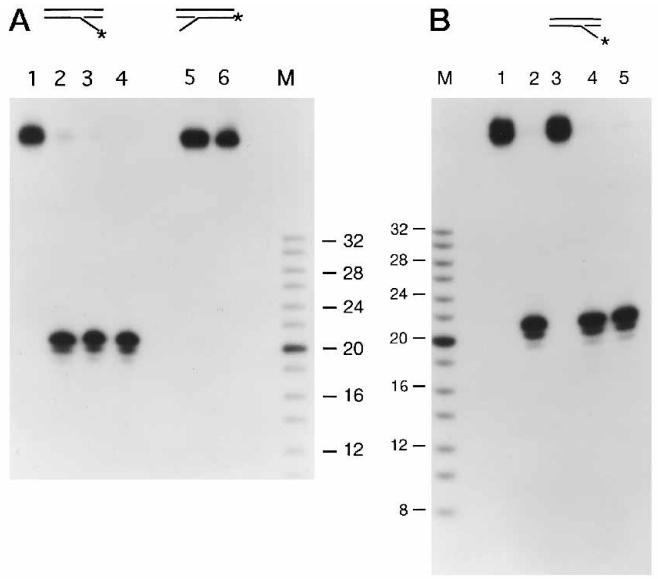

FIG. 3. **Rad2 also acts on 5′-overhanging single-stranded tail in flap DNA.** *A*, cleavage of the flap structure. Flap-1 (*lanes 1–4*) and Flap-2 (*lanes 5* and *6*) DNAs (75 fmol each) were incubated for 10 min at 30 °C without (*lanes 1* and *5*) and with 10 ng (*lane 2*), 15 ng (*lane 3*), and 20 ng (*lanes 4* and *6*) of Rad2 protein. The radiolabeled cleavage products were revealed by autoradiography after electrophoresis of the reaction mixtures. *B*, inhibition of flap cleavage by Rad2 antibodies. The Flap-1 substrate (75 fmol; *lanes 1–5*) was incubated with 20 ng of Rad2 protein for 10 min (*lanes 2–5*) in the presence of 1 μg of affinity-purified antibodies specific for Rad2 (*lane 3*), Rad1 (*lane 4*), or Rad10 (*lane 5*). The positions in nucleotides of the size markers are shown in *lane M*.

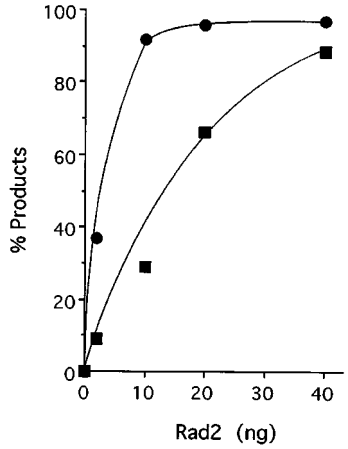

FIG. 4. **Rad2 cleaves flap structures more efficiently than pseudo Y.** Pseudo Y-1 and Flap-1 DNAs (75 fmol each) were incubated for 10 min at 30 °C with the indicated amounts of Rad2 protein. The gel containing the radiolabeled DNA substrates and cleavage products was analyzed in the PhosphorImager to obtain data for a graphical representation of the results. ■, pseudo Y-1; ●, Flap-1.

structure because (i) no cleavage of oligonucleotide A used in the construction of pseudo Y-1 occurred at the same (Fig. 2, *lane 2*) and higher (data not shown) concentrations of Rad2 protein, and (ii) the 3′-overhanging single strand in a similar DNA structure (pseudo Y-2) that was obtained by hybridizing radiolabeled oligonucleotide E to nonlabeled oligonucleotide A (see Fig. 1 and "Materials and Methods") was not cleaved by Rad2 (Fig. 2, *lane 4*).

Rad2 Nuclease Cleaves Flap DNA Structure—The murine FEN-1 nuclease, a structural homolog of Rad2 protein, does not cleave pseudo Y DNA structures, but acts efficiently on "flap" DNA structures that contain a 5′-overhanging single strand (11), cleaving the 5′-overhanging single-stranded tail in the flap structures at and around the single strand-duplex junction. However, FEN-1 does not act on flap structures that contain a 3′-overhanging single-stranded tail (11). The results presented above indicate that, unlike FEN-1, Rad2 nuclease cleaves pseudo Y DNA efficiently, showing specificity for the 5′-overhanging single strand in pseudo Y (Fig. 2). To investigate whether Rad2 also cleaves flap DNA, we hybridized 5′-^{32}P-labeled oligonucleotide C to nonradiolabeled oligonucleotides A and B to form the Flap-1 substrate, which contains a 20-nucleotide 5′-overhanging single strand (Fig. 1), and we also hybridized 5′-radiolabeled oligonucleotide E to nonlabeled oligonucleotides A and D to form the Flap-2 structure, which contains a 3′-overhanging single strand (Fig. 1). The two flap substrates were then incubated with Rad2 protein under reaction conditions employed for the cleavage of pseudo Y-1. As shown in Fig. 3*A*, Rad2 protein cleaved Flap-1 highly efficiently, yielding a major product of 21 nucleotides (≈74%), a lesser product of 20 nucleotides (≈21%), and a trace of a product of 19 nucleotides (≈5%). From the sizes of the cleavage products, it could be deduced that the major site of cleavage is located at 1 base inside the duplex region, and the minor sites are at the single strand-duplex junction and 1 base into the single-stranded region (see Fig. 6). In contrast, no cleavage of the 3′-overhanging single strand in Flap-2 was detected at the highest amount of Rad2 protein under the same reaction conditions (Fig. 3*A*, *lane 6*). Thus, the Rad2 flap cleaving activity closely resembles that of the FEN-1 protein in showing specificity for a 5′-overhanging single strand only.

The Flap-1 and pseudo Y-1 cleaving activities are intrinsic to Rad2 protein because (i) the Rad2 protein used in this study is essentially homogeneous, and (ii) the cleavage of Flap-1 (Fig. 3*B*) and pseudo Y-1 (data not shown) was strongly inhibited by affinity-purified antibodies raised against Rad2 protein (compare *lanes 3* and *2*) expressed in and purified from *E. coli* (14), but it was unaffected by antibodies specific for Rad1 and Rad10 proteins (*lanes 4* and *5*).

Rad2 Cleaves Flap Structures More Efficiently than Pseudo Y—The results presented in Figs. 2 and 3 indicate that Rad2 nuclease acts on the 5′-overhanging single-stranded tail in both pseudo Y and flap structures. Since Flap-1 differs from pseudo Y-1 only in possessing oligonucleotide B, which is the exact complement of the 3′-overhanging single strand in the latter, a direct and meaningful comparison of the relative cleavage efficiencies of the two classes of DNA structure was possible. Since ^{32}P-labeled oligonucleotide C was common to pseudo Y-1 and Flap-1, the two DNA structures used in the comparison had the same molar specific radioactivity. As shown in Fig. 4, the Flap-1 substrate was cleaved by Rad2 protein at a significantly higher efficiency than was pseudo Y-1. For instance, whereas ≈90% of Flap-1 was cleaved by 10 ng of Rad2 protein, ≈30% of pseudo Y-1 was cleaved by the same quantity of Rad2 (Fig. 4). The conclusion regarding the relative activities of Rad2 protein on the pseudo Y and flap structures was validated in at least three other independent experiments (data not shown).

The DNA structure-specific nuclease activity of Rad2, as assayed using Flap-1 DNA as substrate, requires Mg^{2+}, which cannot be replaced by Ca^{2+}, Co^{2+}, Cu^{2+}, or Zn^{2+}, although Mn^{2+} is partially effective (Table I). The flap cleavage activity is not affected by KCl concentrations up to 50 mM, but higher amounts of the salt result in significant inhibition of the activity (data not shown), and the activity is abolished by 0.1% SDS (Table I).

Cleavage of 5′-Overhanging Single Strand in "Bubble" Structure—To investigate whether Rad2 nuclease would act on a single-stranded region located in a bubble structure, we hybridized ^{32}P-labeled oligonucleotide G to nonlabeled oligonucleotide

TABLE I
Effect of divalent metal ions on Rad2-mediated flap cleavage

Flap-1 DNA (75 fmol) was incubated for 10 min at 30 °C with 7.5 ng of Rad2 protein and 5 mM $MgCl_2$ in the complete reaction or with a 5 mM concentration of the chloride salt of one of the indicated divalent metals in the absence of $MgCl_2$. After electrophoresis, the cleavage products were quantified in the PhosphorImager; 100% activity corresponds to conversion of 70% of Flap-1 to products. The cleavage pattern in the presence of Mn^{2+} was the same as that of Mg^{2+} (data not shown).

Reaction components	Activity
	%
Complete reaction	100
Complete reaction + 0.1% SDS	<0.5
$-Mg^{2+}$	<0.5
$-Mg^{2+}$, $+Mn^{2+}$	24
$-Mg^{2+}$, $+Ca^{2+}$	<0.5
$-Mg^{2+}$, $+Co^{2+}$	<0.5
$-Mg^{2+}$, $+Cu^{2+}$	<0.5
$-Mg^{2+}$, $+Zn^{2+}$	<0.5

F to yield a bubble substrate that contains unpaired single-stranded regions 14 bases in length (Fig. 1). The bubble DNA was incubated with increasing concentrations of Rad2 protein under standard conditions, along with the same molar amount of pseudo Y-1 and Flap-1 for comparison. As shown in Fig. 5, there was a Rad2 protein concentration-dependent cleavage of the bubble DNA. The product of Rad2 nuclease action was 39 nucleotides in length, indicating that the incision site is located at 1 base into the duplex region that is proximal to the 3′-end of the labeled strand in the bubble DNA (Fig. 6). In this (Fig. 5) and three other independent experiments (data not shown), Rad2 protein acted with a lower efficiency on the bubble structure than on either pseudo Y-1 or Flap-1. Whether this lower efficiency is related to the DNA structure and/or is due to a DNA sequence effect is not clear at present. However, the results obtained with the bubble DNA indicate that Rad2 nuclease acts on the single strand-duplex DNA junction in the absence of a free end in the single strand.

DISCUSSION

Our work indicates that Rad2 cleaves flap and pseudo Y structures and that it is more active in cleaving flap structures than pseudo Y. In this regard, Rad2 resembles the mammalian FEN-1 and *S. cerevisiae* RTH1 nucleases, which are also more efficient at cleaving flap structures than pseudo Y (11). A variety of experiments have indicated that the *E. coli* pol I 5′ → 3′ exonuclease gains access to the cleavage site by moving from the free 5′-end of single-stranded DNA to the site of cleavage at the junction with duplex DNA (5). Biochemical studies of FEN-1 and calf thymus 5′ → 3′ exonuclease have indicated a similar requirement for a free 5′-end for strand cleavage to occur.[3] In agreement with these observations, we find no cleavage of bubble structure by the *S. cerevisiae* RTH1 protein that we have purified to near homogeneity (data not shown). Unlike RTH1 and FEN-1 nucleases, Rad2 cleaves the bubble structure, albeit with a lower efficiency than the flap or pseudo Y structure. The differential ability of Rad2 and RTH1 proteins to cleave bubble DNA may reflect the affinity of these proteins for binding bubble DNA. Rad2 may possess a domain that confers the ability to bind bubble DNA, and the inability of RTH1 to cleave bubble DNA may arise from the absence of this domain.

The ability of FEN-1/RTH1 to cleave 5′-end single-stranded DNA at its junction with duplex DNA has led to the suggestion that Rad2 cleaves the damaged DNA strand on the 3′-side of the damage during NER (11). While the manner of cleavage of model DNA substrates by Rad2 reported in our present work

[3] R. Bambara, personal communication.

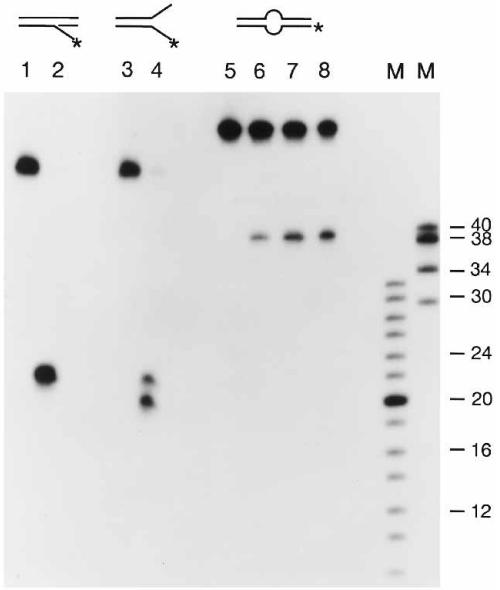

FIG. 5. **Cleavage of bubble DNA structure by Rad2.** Flap-1 (*lanes 1* and *2*), pseudo Y-1 (*lanes 3* and *4*), and bubble (*lanes 5–8*) DNAs (75 fmol each) were incubated for 10 min at 30 °C without (*lanes 1*, *3*, and *5*) or with 20 ng (*lane 6*), 30 ng (*lanes 2*, *4*, and *7*), and 40 ng (*lane 8*) of Rad2 protein. PhosphorImager analysis revealed 17% (*lane 6*), 27% (*lane 7*), and 33% (*lane 8*) cleavage of the bubble DNA, ~90% cleavage of the pseudo Y-1 (*lane 4*), and >90% cleavage of the Flap-1 (*lane 2*) substrates. The positions in nucleotides of the size markers used are shown in the *M lanes*.

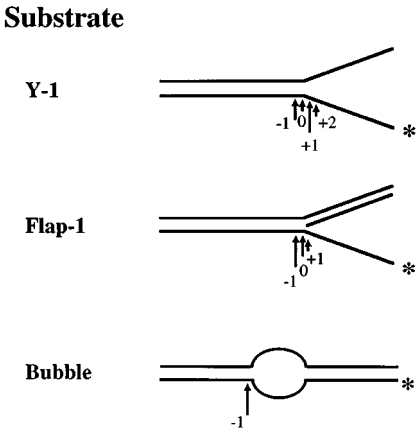

FIG. 6. **Summary of cleavage sites in DNA substrates.** The numbers *−1*, *0*, *+1*, and *+2* indicate cleavage sites 1 base into the duplex region, at the single strand-duplex junction, 1 base into the single-stranded region, and 2 bases into the single-stranded region, respectively.

and by Rad1-Rad10 reported by Bardwell *et al.* (16) is congruent with the proposal that these proteins incise the damaged DNA strand on the 3′- and 5′-sides of the damage, respectively, direct evidence demonstrating this cleavage pattern in NER is as yet unavailable. Since neither the Rad2 nor Rad1-Rad10 nuclease has any affinity for damaged DNA (14, 17, 18), they must be targeted to the damage site via interaction with the damage recognition factors. The interaction of human XPA with the ERCC1 protein (19, 20) would suggest that the Rad1-Rad10 nuclease is targeted to the damage site via interaction with the damage recognition protein Rad14. Interaction with the other components of the NER machinery may target Rad2 to the damage site. It remains to be determined whether the site of placement of the Rad1-Rad10 and Rad2 nucleases on the damaged DNA strand is coincident with the cleavage pattern of these enzymes on model DNA substrates. The recent reconsti-

tution of the incision step of NER with purified components in yeast (3) should make it feasible to ascertain the manner of assembly and the site of cleavage by these nucleases.

Acknowledgment—We thank R. Bambara for sharing with us results on FEN-1.

REFERENCES

1. Huang, J. C., Svoboda, D. L., Reardon, J. T., and Sancar, A. (1992) *Proc. Natl. Acad. Sci. U. S. A.* **89,** 3664–3668
2. Prakash, S., Sung, P., and Prakash, L. (1993) *Annu. Rev. Genet.* **27,** 33–70
3. Guzder, S. N., Habraken, Y., Sung, P., Prakash, L., and Prakash, S. (1995) *J. Biol. Chem.* **270,** 12973–12976
4. Konrad, E. B., and Lehman, I. R. (1974) *Proc. Natl. Acad. Sci. U. S. A.* **71,** 2048–2051
5. Lyamichev, V., Brow, M. A. D., and Dahlberg, J. E. (1993) *Science* **260,** 778–783
6. Goulian, M., Richards, S. H., Heard, C. J., and Bigsby, B. M. (1990) *J. Biol. Chem.* **265,** 18461–18471
7. Ishimi, Y., Claude, A., Bullock, P., and Hurwitz, J. (1988) *J. Biol. Chem.* **263,** 19723–19733
8. Turchi, J. J., and Bambara, R. A. (1993) *J. Biol. Chem.* **268,** 15136–15141
9. Turchi, J. J., Huang, L., Murante, R. S., Kim, Y., and Bambara, R. A. (1994) *Proc. Natl. Acad. Sci. U. S. A.* **91,** 9803–9807
10. Waga, S., Bauer, G., and Stillman, B. (1994) *J. Biol. Chem.* **269,** 10923–10934
11. Harrington, J. J., and Lieber, M. R. (1994) *Genes & Dev.* **8,** 1344–1355
12. Sommers, C. H., Miller, E. J., Dujon, B., Prakash, S., and Prakash, L. (1995) *J. Biol. Chem.* **270,** 4193–4196
13. Johnson, R. E., Kovvali, G. K., Prakash, L., and Prakash, S. (1995) *Science* **269,** 238–240
14. Habraken, Y., Sung, P., Prakash, L., and Prakash, S. (1993) *Nature* **366,** 365–368
15. Bailly, V., Sommers, C. H., Sung, P., Prakash, L., and Prakash, S. (1992) *Proc. Natl. Acad. Sci. U. S. A.* **89,** 8273–8277
16. Bardwell, A. J., Bardwell, L., Tomkinson, A. E., and Friedberg, E. C. (1994) *Science* **265,** 2082–2085
17. Sung, P., Prakash, L., and Prakash, S. (1992) *Nature* **355,** 743–745
18. Sung, P., Reynolds, P., Prakash, L., and Prakash, S. (1993) *J. Biol. Chem.* **268,** 26391–26399
19. Li, L., Elledge, S. J., Peterson, C. A., Bales, E. S., and Legerski, R. J. (1994) *Proc. Natl. Acad. Sci. U. S. A.* **91,** 5012–5016
20. Park, C.-H., and Sancar, A. (1994) *Proc. Natl. Acad. Sci. U. S. A.* **91,** 5017–5021